Macromolecules (structure)

J. Stellbrink

This document has been published in

Thomas Brückel, Gernot Heger, Dieter Richter, Georg Roth and Reiner Zorn (Eds.):
Lectures of the JCNS Laboratory Course held at Forschungszentrum Jülich and the research reactor FRM II of TU Munich
In cooperation with RWTH Aachen and University of Münster
Schriften des Forschungszentrums Jülich / Reihe Schlüsseltechnologien / Key Technologies, Vol. 39
JCNS, RWTH Aachen, University of Münster
Forschungszentrum Jülich GmbH, 52425 Jülich, Germany, 2012
ISBN: 978-3-89336-789-4

6 Macromolecules (structure)

J. Stellbrink
Jülich Centre for Neutron Science 1
Forschungszentrum Jülich GmbH

Contents

6.1 Introduction 2

6.2 Polymers in dilute solution 2

6.2.1 Linear polymers 2
6.2.2 Branched polymers 5
6.2.3 In-situ experiments during polymerisation 7

6.3 Block copolymer Micelles 9

6.3.1 Form factor 9
6.3.2 Micellar exchange dynamics 10
6.3.3 Structure factor 11

6.4 Soft Colloids 12

Appendices 14

References 15

Exercises 16

Lecture Notes of the JCNS Laboratory Course Neutron Scattering

6.1 Introduction

Macromolecules are an integral part of Soft and Living Matter. In *Living Matter*, macromolecule-based functional systems are built from molecular units consisting of only a few different building blocks: amino acids are assembled into proteins, which in turn function individually, or cooperatively in nano- and micro-machines. The secret of success is the intrinsic hierarchical structuring over a large range of length scales. In *Soft Matter*, synthetic macromolecules are of much simpler structure. Nevertheless, there is a vast variety of material properties that can be realized with synthetic macromolecules. Theoretical concepts have been developed, and are essential for the rational design of soft materials, that are of paramount importance in a multitude of technical applications.

Synthetic polymers have crucially changed daily life since its development in the 1930ies. Modern polymers can be divided into two major classes (i) commodity polymers for daily life use which are produced in millions of tons per year and (ii) specialty polymers for high-performance applications which are niche products but highly profitable [1]. Typical commodity polymers are polyolefines like polyethylene (PE) or polypropylene (PP) used for packaging, films etc. Examples for specialty polymers are polydimethylsiloxane (PDMS) derivatives used in dental implants.

Currently, both classes of polymers in use are based on petrochemical feedstock, thus considered not "carbon-neutral" and "environment-friendly". Due to changing global conditions and growing concerns about the mounting disposal problems, research on sustainable commodity polymers has been intensified during the last decade, both on the level of fundamental research and applied science [2]. To find the required balance between material properties and bioavailability/-degradability is the key for establishing sustainable polymers on a large scale industrial level and therefore a major challenge of future polymer science.

The development of new biomimetic specialty polymers is another major challenge. Biopolymers, like spider silk, are high-performance materials with material properties superior to any synthetic polymer. To transfer these properties to artificial biomimetic polymers, one has to fully understand, on the molecular level, the structure-property-relationships and enzymatic synthesis processes in living organisms.

In this lecture some recent applications of neutron scattering methods to characterize quantitatively on a microscopic length scale structure and interactions of synthetic macromolecules and its hierarchical structuring are given. A more comprehensive overview is found e.g. in [3].

6.2 Polymers in dilute solution

6.2.1 Linear polymers

A linear polymer is a sequence of molecular repetition units, the monomers, continuously linked by covalent bonds. The degree of polymerisation, D_p, i.e. the number of monomers constituting the polymer, the (weight average) molecular weight, $M_w=D_p\,M_m$, with M_m the molecular weight of the monomer, and the radius of gyration, $R_g \sim M_w^{\nu}$, are the most important structural parameters of a polymer. On a coarse grained level, structural details arising from the explicit chemical composition of the

polymer like bond lengths and angles can be neglected and what remains is the so called scaling relation given above that links molecular weight to size and which is generally valid for all polymers [4]. The numerical value of the scaling exponent ν depends on the strength of interactions. In the so called θ-state, when monomer-monomer interactions are as strong as monomer solvent interactions, the polymer structure can be described by a random walk, therefore Gaussian chain statistics are valid and ν=1/2, see Chapter 5.3.3. When monomer solvent interactions are stronger than monomer-monomer interactions, so called excluded volume forces are effective, the polymer chain is "swollen" and ν=3/5.

Here one has to emphasize that synthetic polymers, unlike biopolymers, always have an intrinsic polydispersity, i.e. there is a distribution of molecular weights. The polydispersity is given usually in terms of M_w/M_n, with M_n the number average molecular weight. Its precise number depends on the polymerisation reaction by which the polymer was synthesized. For a (theoretical) monodisperse polymer M_w/M_n=1 holds, the most monodisperse synthetic polymers with M_w/M_n=1.02 can be synthesized by "living" anionic polymerisation, classical polycondensation yields M_w/M_n =2, radical polymerisation can even result in extremely broad distributions, M_w/M_n >10.

Although in technical applications polymers are mostly used as bulk materials, polymer characterisation is usually performed in (dilute) solution. Historically, light scattering was the method of choice to characterise synthetic polymers [5], but nowadays size exclusion chromatography (SEC), also called gel permeation chromatography (GPC), is the standard technique to characterize routinely polymers [6].

Neutron scattering, due do its limited accessibility and high experimental costs, usually is found in basic academic research, but here it played a crucial role in confirming fundamental theoretical concepts of polymers [3].

As explained in detail in Chapter 5.3.4 the measured intensity $I(Q)=P(Q)\,S(Q)$ is in first approximation a product of particle form factor $P(Q)$ given by the *intra*molecular structure, i.e. the particle shape, and structure factor $S(Q)$ given by the *inter*molecular structure arising due to particle-particle interactions. To characterize properly the *intra*molecular form factor $P(Q)$ one has therefore to investigate a concentration series in the dilute regime and extrapolate finally to infinite dilution. The form factor of a Gaussian chain (Debeye function) has been derived in Chapter 5.3.3.

Particle-particle interactions as seen in $S(Q)$ are weak in the dilute regime, but still effective, so that one can apply the virial expansion.

$$\phi / I(Q=0) = 1/V_w + 2A_2\phi + \ldots \tag{6.1}$$

Here ϕ is the polymer volume fraction and $V_w = M_w/d$ is the molecular volume and d the polymer density in [g/cm^3]. The value of the second virial coefficient A_2 directly reflects particle-particle interactions, i.e. a positive A_2 is found for repulsive interactions (good solvent), a negative one for attractive interactions (marginal/bad solvent) and finally A_2=0 characterizes no interactions (θ-solvent). Without any data fitting this distinction can easily be made by plotting the intensity data $I(Q)$ of a concentration series normalized to the corresponding volume fractions $I(Q)/\phi$ (Since scattering arises due to an exchange of a volume element of solvent by a volume element of polymer with different scattering contrast, the natural concentration unit for any scattering

experiment should be volume fraction ϕ). This is schematically shown in Figure 6.1. If no particle-particle interactions are present all data for all Q-vectors exactly fall on top of each other.

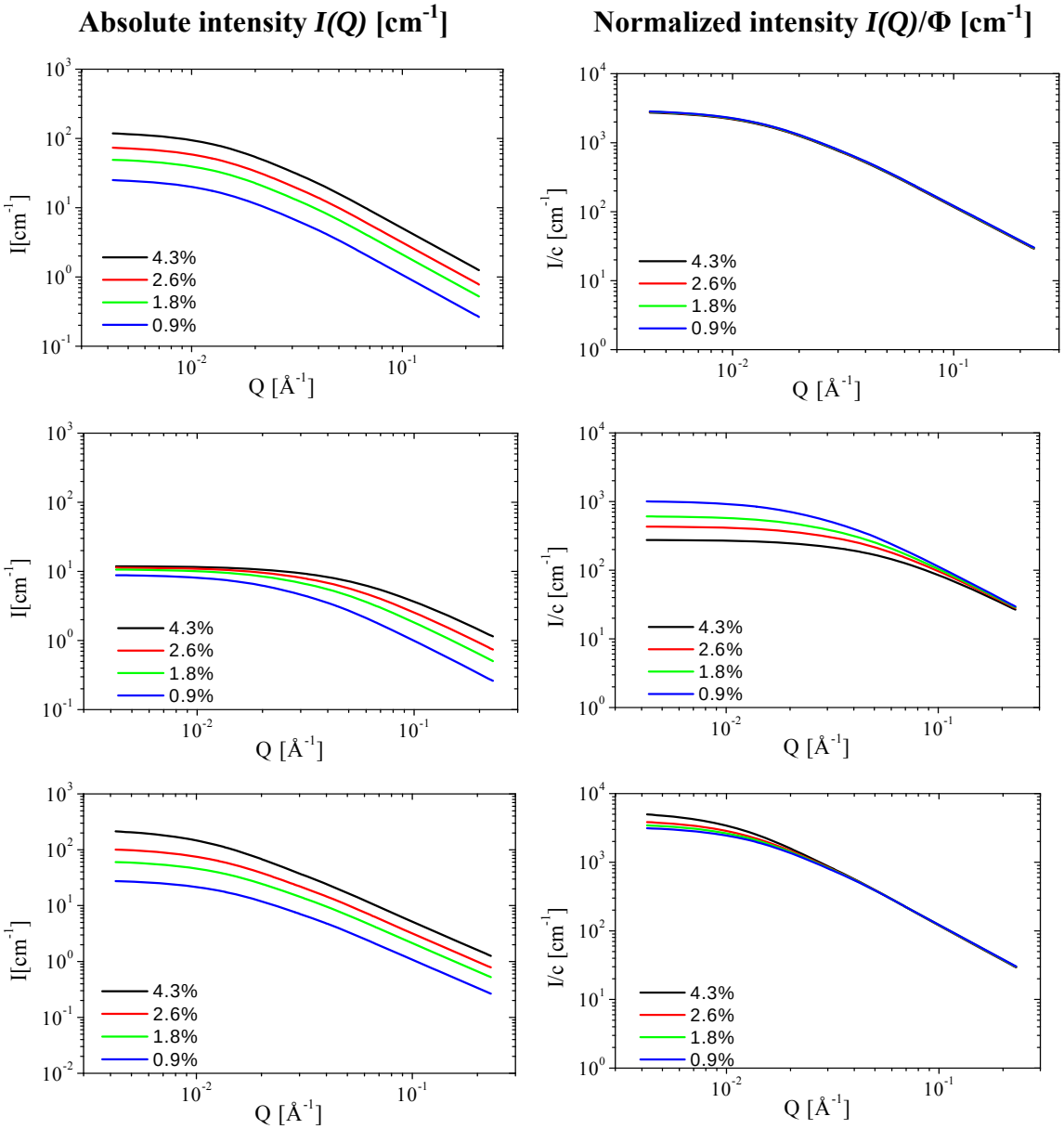

Fig. 6.1: Calculated scattering intensities in absolute units I(Q) (left) and normalized to polymer volume fraction I(Q)/ ϕ (right) for solutions of a linear polymer at different volume fractions given in percent, see legends, assuming a virial ansatz for particle interactions. From top to bottom: No interactions A_2=0 (θ solvent, repulsive interactions A_2>0 good solvent, attractive interactions A_2<0 marginal or bad solvent).

Irrespective what kind of interactions are present this also holds for high Q-vectors, since high Q-vectors mean small length scales and the local (*intra*molecular) structure is not affected by particle-particle interaction ($S(Q)$=1). In contrary, at low Q-vectors there are crucial differences between the individual concentrations in this representation. For

repulsive interactions the forward scattering is reduced by *S(Q)* therefore the lowest concentration shows the highest normalized intensity. For attractive interactions, on the other hand, the forward scattering is increased by *S(Q)*, therefore the lowest concentration shows the lowest normalized intensity. This sequence can be easily understood, because attractive interactions finally result in clustering of the individual particles.

For more details about synthesis and characterisation of macromolecules the interested reader is referred to standard textbooks e.g. [7][8].

6.2.2 Branched polymers

Branching crucially influences the mechanical properties of polymers therefore characterisation and control of branching reactions during polymerisation processes are of vital interest not only for polymer industry to tune semi-empirically material properties, but also for fundamental research to derive a proper quantitative structure property relationship.

The simplest branched polymer is a regular star polymer, where *f* arms, each of same molecular weight $M_{w,arm}$, are emanating from a microscopic central branch point, the star core. Experimentally, such regular star polymers are nowadays most precisely realized by using chlorosilane dendrimers as branch points. The arms forming the star corona or shell are grafted to the dendrimer core by "living" anionic polymerisation [9]. The precise control of the dendrimer generation is reflected in the precise functionality of the final star polymer so that functionalities as high as *f*=128 can be achieved. However, with increasing functionality there is a polydispersity in functionality since the last arms are extremely difficult to graft since they have to diffuse through the already very crowded star polymer corona to react at the star core [10].

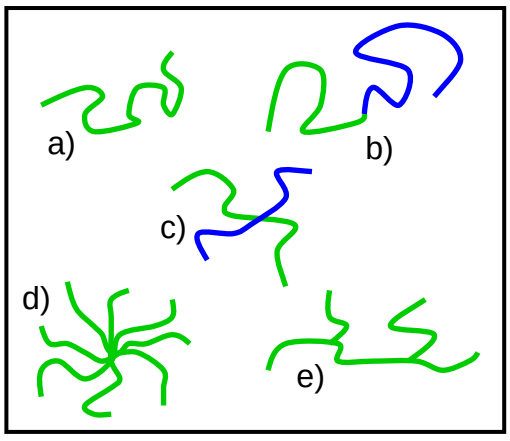

Fig. 6.2: *Schematic illustration of different polymer architectures: a) linear homopolymer, b) linear block copolymer, c) regular mikto-arm star polymer (f=4), d) regular star polymer(f=8), and e) comb polymer.*

The form factor of a regular star polymer with Gaussian chain statistics has been derived by Benoit already in 1953 [11].

$$P_{star}(Q) = \frac{2}{f_w Q^4 R_{g,arm}^4} \times \left[Q^2 R_{g,arm}^2 - \left(1 - e^{-Q^2 R_{g,arm}^2}\right) + \frac{f_w - 1}{2}\left(1 - e^{-Q^2 R_{g,arm}^2}\right)^2 \right] \quad (6.2)$$

The overall size of the star polymer $R_{g,star}$ is related to the size of the individual arm by $R_{g,star} = \sqrt{\frac{(3f-2)}{f}}\, R_{g,arm}$.

There is no rigorous analytical formula for a star polymer with swollen chain statistics, but experimental data for star polymers in a good solvent can be nicely described either by the Dozier function [12] or the approach derived by Beaucage [13]. His equation can be viewed as a "universal form factor" for an arbitrary mass fractal that can also be applied to many other polymeric systems:

$$P(Q) = G \cdot \exp(-Q^2 R_g^2 / 3) + B\left(\frac{1}{Q^*}\right)^P \quad (6.3)$$

with $Q^* = Q/[erf(QkR_g/\sqrt{6})]^3$. Here *erf* is the error function and G and B are amplitudes, which for mass fractals can be related to each other by $B = G \cdot P / R_g^P \cdot \Gamma(P)$ (polymeric constraint). P is the fractal dimension of the internal substructure, k an empirical constant found to be ≈ 1.06 and Γ is the Gamma function. The fractal dimension is related to the scaling exponent by P=1/ν. The Beaucage expression can be nicely extended to describe hierarchically structures over multiple levels *i* $P(Q) = \sum_i P_i(Q)$ where $P_i(Q)$ are given by Equation (6.3).

Fig. 6.3: shows form factors obtained for polybutadiene (PB) star polymers with varying functionality *f* but same R_g≈50nm in d-cis-decalin.

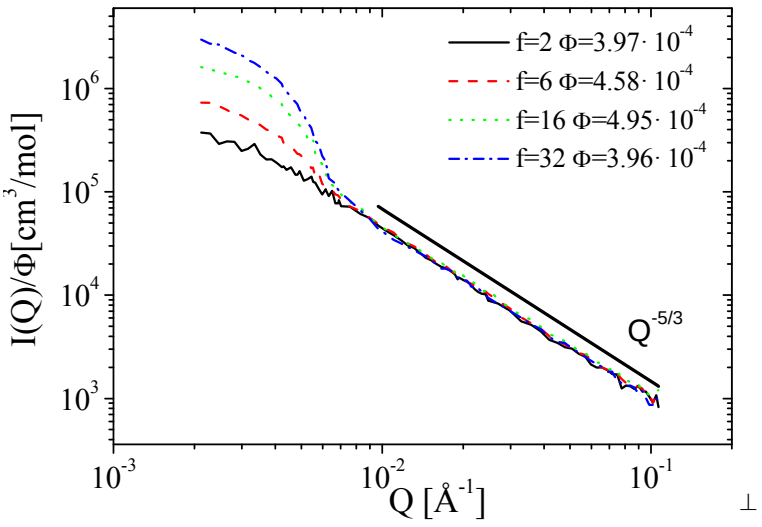

Fig. 6.3: *SANS intensity I(Q) normalized by volume fraction ϕ for regular polybutadiene star polymers with varying functionality f but same radius of gyration R_g≈50nm. The asymptotic power law observed at high scattering vectors $I \sim Q^{-5/3}$ clearly indicates excluded volume interactions relevant in a good solvent , i.e. swollen chain statistics; figure taken from [14].*

At low Q-vectors, $Q \leq 8\times10^{-3}$ Å^{-1}, data could be modelled using the Benoit form factor, Equation (6.2) for a Gaussian star, which gives the explicit dependence on functionality f. For describing the complete data sets we used the Beaucage form factor, Equation (6.3), which describes also the observed power law at high Q-vectors. One should note that this power law extends over more than one order of magnitude in Q and starts at the same Q-value of $\approx 8\times10^{-3}$ Å^{-1} for all f due to the same R_g. The observed power law slope of $I(Q) \sim Q^{-5/3}$ reflects the good solvent quality of cis-decaline for polybutadiene and decreases slightly with increasing f, indicating increasing arm stretching due to the increasing monomer density in the star corona.

The effect of branching becomes easily visible by using a so called Kratky representation, $I(Q)\ Q^2$ vs. Q. Whereas a linear polymer with Gaussian chain statistics reaches monotonically an asymptotic plateau, any branched structure shows a maximum. For the here discussed regular star polymer the height quantitatively depends on the arm number or functionality f, see Fig. 6.4:

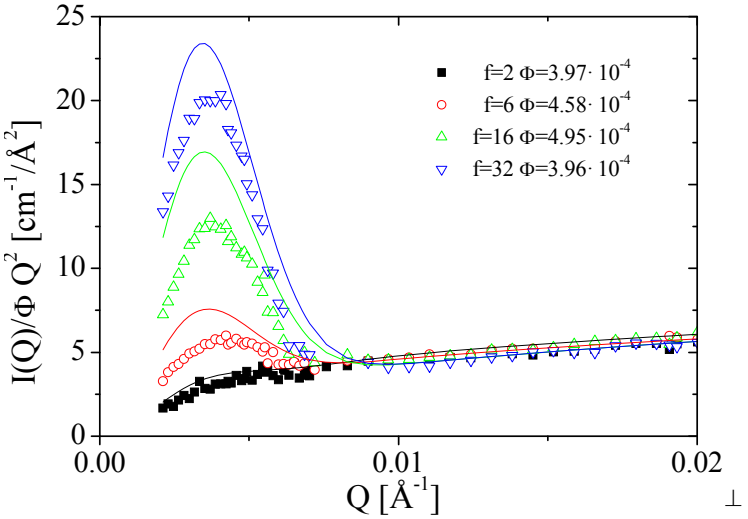

Fig. 6.4: *Kratky representation $I(Q)\ Q^2$ vs. Q for same data as in Fig. 6.3. The increasing peak height with increasing functionality f due to branching becomes clearly visible as well as the discrepancy between experimental data (symbols) and Beaucage function used to model the data. The fact that no asymptotic plateau is observed results from the excluded volume interactions relevant in a good solvent, i.e. swollen chain statistics.*

6.2.3 In-situ experiments during polymerisation

For understanding and controlling any chemical reaction a detailed understanding of reaction mechanism, type and role of intermediate species as well as reaction kinetics are prerequisite. How the microscopic structure of a growing polymer chain is evolving in the different steps of polymerisation reactions has to be resolved by non-invasive, real-time measurements. The ideal tool is small angle neutron scattering (SANS), since the microscopic structure of polymer-based materials can be resolved on a micrometer-to- nanometer-level by modern neutron scattering techniques. In addition, contrast variation, i.e. H/D exchange, can even "stain" certain parts of the polymers giving

access to unprecedented structural information. So neutron scattering is a unique and outstanding technique to investigate polymerising systems in real-time, in particular since new, more powerful neutron sources became available worldwide (FRM-2, SNS, J-PARC). But for a complete description of the polymerisation process additional information in terms of reaction kinetics etc. are prerequisite. Thus, in-situ SANS experiments have to be supported by complementary methods like NMR, SEC, UV/VIS and IR spectroscopy, favourably also in real-time mode.
Recently we investigated reaction mechanism and kinetics of different polymerisation techniques like "living" anionic polymerisation [15] or post-metallocene catalyzed olefin polymerisation [16] by such an in-situ multi technique approach. Fig. 6.5: shows time resolved SANS intensities *I(Q)* in absolute units obtained during the polymerisation of 1-octene by a pyridylamidohafnium catalyst in toluene at 20°C. Experiments have been performed using the KWS-1 instruments at the former FRJ-2 reactor in Jülich which allowed a temporal resolution of about several minutes.

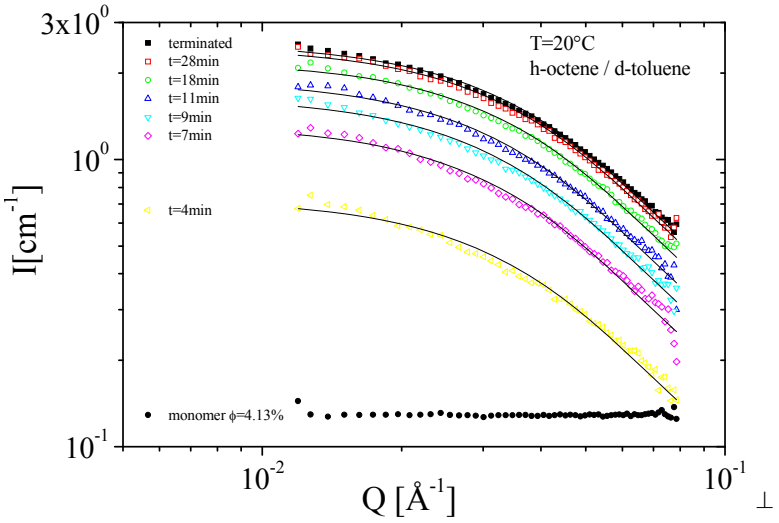

Fig. 6.5: *Time resolved SANS intensities I(Q) in absolute units obtained during the polymerisation of 1-octene by a pyridylamidohafnium catalyst in toluene at 20°C; figure taken from [16].*

Whereas the monomer solution shows a *Q*-independent intensity over the whole accessible SANS *Q*-range typical for small molecules ("incoherent scatterers"), after 4 minutes a polymer is already formed and the *Q*-dependence of the intensity can be described by a Beaucage form factor, Equation (6.3). With ongoing polymerisation, increasing polymerisation time *t* the general shape of *I(Q)* does not change any further, only the forward scattering *I(Q=0)* is increasing due to the increasing molecular weight and concentration of the growing polymer chain. Finally, the polymerisation is almost finished after half an hour as can be seen by comparison with the terminated polymer. A detailed quantitative analysis of *I(Q,t)* reveals that during this type of polymerisation reaction no aggregation phenomena of the growing polymer chain are relevant. Similar experiments at high flux sources allow today temporal resolutions smaller than 1 second if experiments are repetitively performed using a stopped flow mixer.

6.3 Block copolymer Micelles

When amphiphilic block copolymers are dissolved in a selective solvent, i.e. a solvent which is good for one block but a precipitant for the other, they spontaneously self-assemble into supramolecular aggregates known as micelles, in which the insoluble block forms the inner part or core, whereas the soluble block forms a solvent-rich shell or corona. The general behaviour of block copolymers in selective solvents has been subject of copious theoretical and experimental studies during the past decades. They are reviewed in several books [17] [18] and review articles [19][20] related to this topic.
Extensive studies demonstrated that the micellar morphology can be tuned (going from spheres, cylinders, worms and vesicles) by varying the block-copolymer molecular weight, the chemical nature and the ratio of the blocks. One of the most extensively studied block-copolymers is poly(butadiene-ethylene oxide) (PB-PEO). As a function of the hydrophilic block length (in term of PEO weight fraction w_{PEO}) spherical micelles ($w_{PEO} > 0.6$), worm-like micelles, WLM ($0.47 \leq w_{PEO} \leq 0.59$) or bilayers ($w_{PEO} < 0.47$) are formed. Different theoretical studies contributed to define the scaling laws for the parameters of equilibrium structures. Among them, a quantitative theory defining the thermodynamic stability of different morphologies in selective solvents has been recently developed [21]. The theory expresses the free energy contributions of the core, the corona and the interface as a function of the blocks structural parameters and the interfacial tension between the solvent and the insoluble block for different micellar morphologies. Solvent selectivity can be more easily tuned than the above mentioned parameters (molecular weight, block ratio etc) and moreover in a continuous way by varying the solvent composition. Therefore solvent composition is a very natural and easy parameter to control the micellar structures. The change in the morphology of the self-assembled structures can be attributed to a change of solvent selectivity, which influences the different energy contributions responsible for the morphology: core-chain stretching, corona-chain repulsion and interfacial tension between the core and the solution.
The interest is to relate changes on the smallest relevant length scale, i.e. diameter and aggregation number per unit length, density profile in the corona, to changes in the macroscopic structure, i.e. the contour and persistence length of wormlike micelles and the transition from wormlike-to-spherical micelles etc. This molecular level understanding can help to elucidate the mechanisms involved in non equilibrium conditions. Besides, it is expected that these quantities have a pronounced effect on the rheological behavior of the systems, and as such solvent composition could be used to tune the flow properties of micellar solutions.

6.3.1 Form factor

Figure 6.6 (left) shows the partial form factor normalized to volume fraction Φ, $P(Q)/\Phi$, in shell and core contrast for micelles formed by a symmetric amphiphilic block copolymer poly(ethylene-alt-propylene)–poly(ethylene oxide), h-PEP4-dh-PEO4 (the numbers denote the block molecular weight in kg/mol) [22]. Already, a qualitative discussion of the data reveals important features of the micellar architecture. First, the forward scatterings, $I(Q = 0)$, in the two contrasts are the same. This is expected for micelles formed by a symmetric diblock copolymer in shell and core contrast (we should note that the two blocks have the same molar volume V_w) and is in this sense a

proof of the applied contrast conditions. This means that the scattering profiles shown in figure 2 are directly reflecting pure shell and core properties. Second, both scattering profiles show well defined maxima and minima, up to 4 in core contrast, which arise from sharp interfaces typical for a monodisperse, compact particle. Also shown is Porod's law $I \sim Q^{-4}$, which describes the limiting envelope of all form factor oscillations. (We should note that one has to consider that these oscillations are already smeared by the instrumental resolution function, so the data shown offer even more confirmation of the strong segregation between the core and corona and the low polydispersity of the micelles.) We should emphasize that in core contrast no *blob* scattering is visible [22]. This also corroborates the compact PEP core. A quantitative analysis in terms of a core–shell model gave the following micellar parameters: aggregation number P = 1600, core radius R_{core} = 145 Å and shell radius R_m = 280 Å with a polydispersity of ≈5%. The solvent fraction in the swollen shell is Φ_{solv} = 60%.
Figure 6.6 (right) shows the corresponding partial form factor data, $P(Q)/\Phi$, in shell and core contrast for an asymmetric h-PEP1-dh-PEO20. The differences compared to figure 6.6. (left) are obvious: the difference in forward scattering of the two contrasts is reflecting the asymmetry of the block copolymer. Moreover, no maxima or minima are visible (also not at high Q in core contrast) and the power law observed in shell contrast has a slope of only $I \sim Q^{-5/3}$, which is typical for a polymer chain in a good solvent and arises from the swelling of the PEO in the shell (*blob* scattering). A quantitative analysis gives the following micellar parameters: aggregation number P = 130, core radius R_{core} = 34 Å and shell radius R_m = 260 Å.

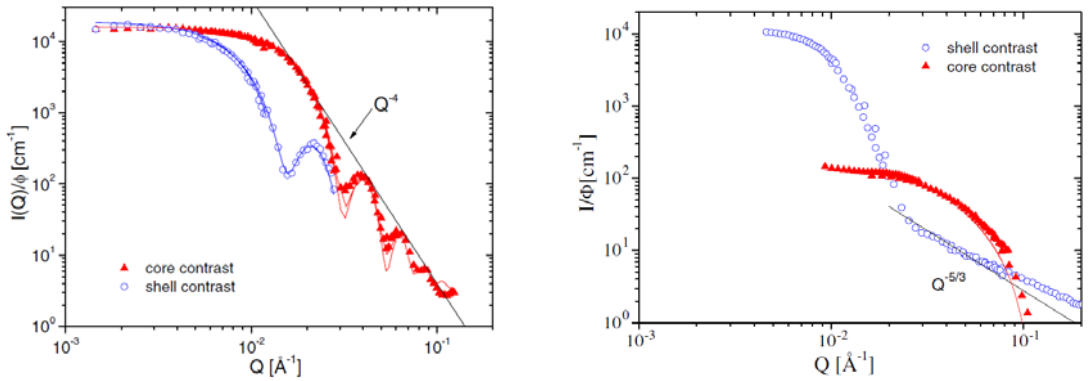

Fig. 6.6: *Form factors of block copolymer micelles with varying architecture in core (red) and shell contrast(blue). Left symmetric PEP4-PEO;right asymmetric PEP1-PEO20, the numbers denote the block molecular weight in kg/mole. Figure taken from [22].*

6.3.2 Micellar exchange dynamics

Polymeric micelles are macromolecular analogues of well-known low-molecular surfactant micelles. As a consequence of random stochastic forces, the constituting chains will continuously exchange between the micelles. From the theory of Halperin and Alexander (HA), this exchange kinetics is expected to be dominated by a simple expulsion or insertion mechanism where single chains (unimers) are required to overcome a defined potential barrier [23]. Higher order kinetics including fusion and

fission is not expected to take place since these mechanisms are neither favored energetically nor entropically [24]. Experimentally, relatively few studies have been devoted to the exchange kinetics of polymeric micelles in equilibrium. This is most likely related to the associated experimental difficulties. Recently, we used a newly developed time resolved small angle neutron scattering (TR-SANS) technique [25]. This technique is perfectly suited for determination of exchange kinetics in equilibrium as, unlike other techniques; virtually no chemical or physical perturbations are imposed on the system. The labeling is restricted to a simple hydrogen/deuterium (H=D) substitution using fully hydrogenated (h) and fully deuterated (d) polymers with identical molar volumes and compositions. By mixing the corresponding H- and D-type micelles in a solvent with a scattering length corresponding to the average between the two, the kinetics can be determined. The average excess fraction of labeled chains residing inside the micelles is then simply proportional to the square root of the excess SANS intensity. The corresponding correlation function is given by $R(t) = \{[I(t) - I_\infty]/[I(t=0) - I_\infty]\}^{1/2}$ was measured from a reference sample where the polymers have been completely randomized and *I(t=0)* from the scattering of the reservoirs at low concentrations.

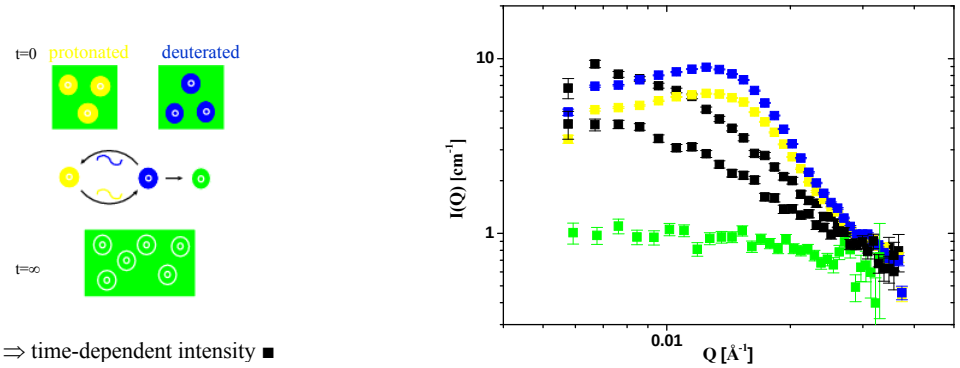

Fig. 6.7: *Left: Schematic illustration of the TR-SANS technique to follow micellar exchange kinetics. Right: Corresponding time-resolved SANS data forPEP1-PEO20 micelles in H2O/DMF 7:3 showing slow exchange (5min, 2h @ 50°C).*

6.3.3 Structure factor

How the structure factor *S(Q)* can be derived from the pair correlation function *g(r)* by liquid state theory has been shown in Chapter 5.3.4. *g(r)* finally results from the effective pair potential *V(r)*, which describes the direct interactions between the solute only, after eliminating the rapidly moving degrees of freedom of the solvent molecules.
We recently showed that micelles formed by the amphiphilic block copolymer poly(ethylene-alt-propylene)– poly(ethylene oxide) (PEP–PEO) provide an interesting system to conveniently tune the 'softness' in terms of particle interactions (intermolecular softness) and the deformability of the individual particle (intramolecular softness). This is achieved by changing the ratio between hydrophobic and hydrophilic blocks from symmetric (1:1, Hard Sphere-like) to very asymmetric (1:20, star-like). One must emphasize that to approach the star-like regime is not a trivial task.
Figure 6.6 compares the effective interaction potential for soft colloids to those of the limiting cases Gaussian Chain, i.e. no interactions, and Hard Spheres, i.e. infinite strength of the potential at contact. The explicit form of *V(r)* for star polymers, the

limiting ultra-soft colloids, was derived by Likos et al. [26] and is explained in detail in Appendix 6.1.

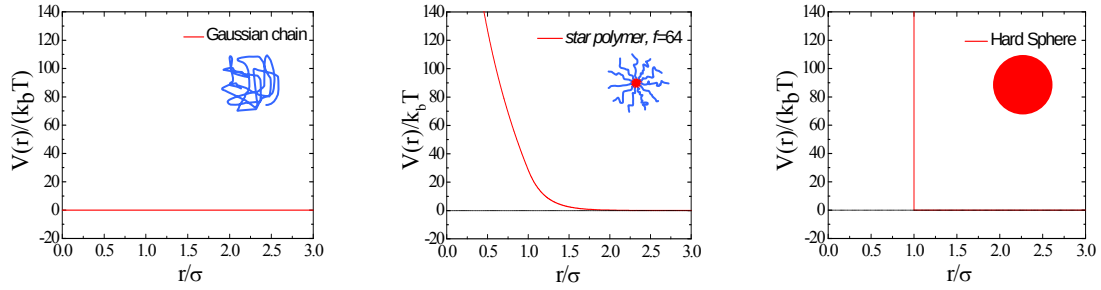

Fig. 6.8: *Different effective interaction potentials. The one for star polymers, i.e. soft colloids, is in-between the two limits Gaussian Chain (left) and Hard Spheres (right).*

Figure 6.9 shows the corresponding experimental structure factors S(Q) for Hard Sphere and Soft interactions and its comparison with theoretical predictions.

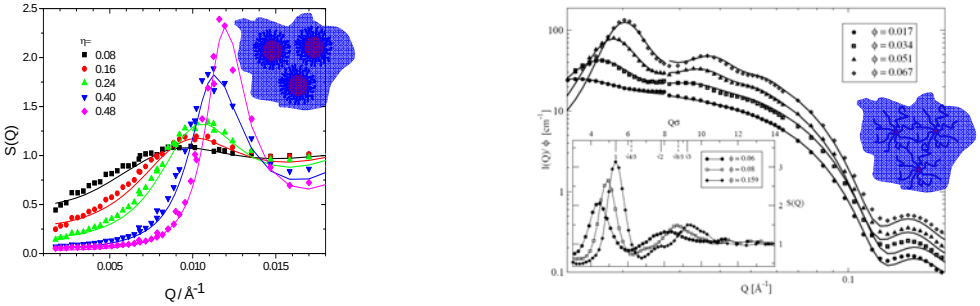

Fig. 6.9: *Experimental structure factor S(Q) of block copolymer micelles with varying architecture obtained by SANS in core contrast (symbols) and the theoretical description (lines) resulting from the corresponding interaction potentials: Symmetric PEP4-PEO4 / Hard Sphere potential left, asymmetric PEP1-PEO20/ ultra soft potential right, see text and [22].*

6.4 Soft Colloids

Soft colloids in general, e.g. polymer-coated silica particles, block copolymer micelles, star polymers etc., are hybrids between (linear) polymer chains and (hard sphere) colloids. Due to this hybrid nature, soft colloids macroscopically show interesting (phase) behaviour resulting from its unique microscopic structure. The combination of polymer-like properties, i.e. the formation of (transient) geometric constraints due to overlapping polymeric coronas and direct colloidal interactions due to the (hard) core in particular affects flow properties and nonequilibrium behaviour of soft colloids. Therefore soft colloids are frequently used in many technical applications (paints, shampoos, motor oils, polymer nano-composites etc.).

More recently, the interest of colloid scientists in fundamental science has shifted towards the study of soft particles, among which star polymers have emerged as a

model system for a wide class of soft spheres. For a star polymer, softness can be controlled by varying its number of arms (or functionality *f*), allowing to bridge the gap between linear polymer Gaussian chains ($f = 2$) and Hard Spheres ($f = \infty$). Therefore, star polymers feature tuneable softness, which is responsible for the observation of anomalous structural behaviour and for the formation of several crystal structures [28]. Hence, mixtures of soft particles offer an even higher versatility with respect to their hard counterparts, both in terms of structural and rheological properties and of effective interactions. Recently, we confirmed experimentally by combining SANS and rheology the theoretical phase diagram of soft colloids [29] and mixtures of soft colloids with linear polymers [29]. As experimental realization again the previously described PEP-PEO star-like micelles have been used. Figure 6.10 shows the phase diagram in the functionality vs. packing fraction representation. We have to point out that quantitative agreement starting from experimental parameters is achieved without any adjustable parameter. For this the determination of the interaction length σ by SANS in core contrast was inevitable.

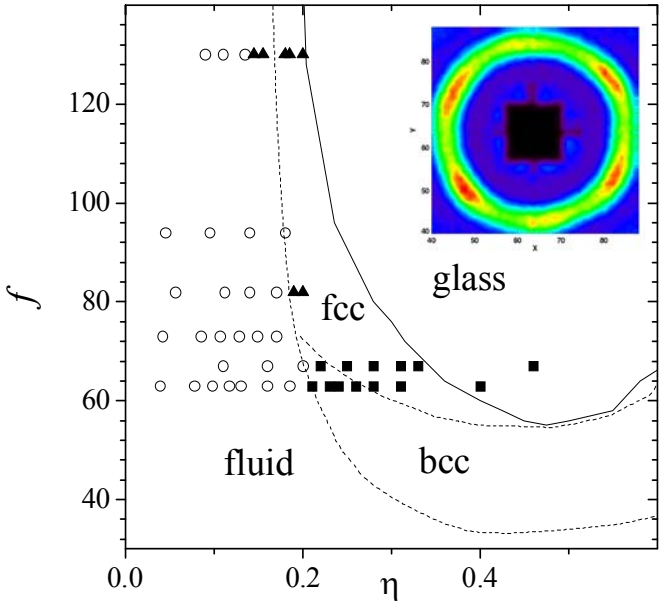

Fig. 6.10: *Phase diagram of ultra soft colloids (symbols experiment: ○ fluid, ■ bcc ▲ amorphous solid;, lines theory). Figure taken from.*

Appendices

A6.1 The ultra-soft potential (Likos-Potential)

The effective potential $V(r)/k_bT$ between star polymers as a function of functionality f and interaction length σ was derived by by Likos et al. [26]. The interaction length σ is the distance between two star centres when the outermost blob overlaps. For larger distances two stars interact via a screened Yukawa-type potential whereas at distances smaller than σ when there is overlap of the star coronas, the potential has an ultra-soft logarithmic form.

$$\frac{V(r)}{k_bT} = \begin{cases} \frac{5}{18} f^{3/2} \left(1+\sqrt{f}/2\right)^{-1} (\sigma/r) \exp\left[-\sqrt{f}\,(r-\sigma)/2\sigma\right] & (r>\sigma) \\ \frac{5}{18} f^{3/2} \left[-\ln(r/\sigma) + \left(1+\sqrt{f}/2\right)^{-1}\right] & (r \le \sigma) \end{cases} \tag{6.4}$$

All numerical factors have been chosen in such a way that the potential as wells as its first derivative are smooth at crossover. Figure 6.11 shows the Likos-potential for different functionalities. At $f = \infty$ the Hard Sphere potential is recovered.

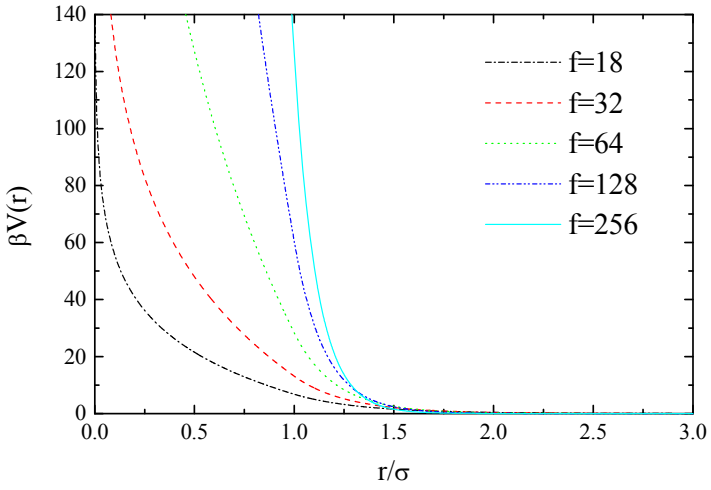

Fig. 6.11: *Effective potential $V(r)/k_bT$ between star polymers with varying functionality f.*

References

[1] C J.R. Severn and J.C. Chadwick, Tailor-Made Polymers, (Wiley-VCH, Weinheim, 2008)
[2] G.W. Coates and M.A. Hillmyer, Polymers from Renewable Resources, Macromolecules, VI2, 7987 (2009); C.K. Williams, M.A. Hillmyer, Polymer Rev. 48, 1 (2008)
[3] J. S. Higgins and H. C. Benoit, Polymers and Neutron Scattering; (Clarendon Press, Oxford, U.K., 1994).
[4] P.G. De Gennes, Scaling Concepts in Polymer Physics, (Cornell University Press, 1979)
[5] W. Brown, Light Scattering: Principles and development, (Oxford University Press, 1996)
[6] S. Mori and H.G. Barth, Size Exclusion Chromatography, (Springer, 1999)
[7] P.J. Flory, Principles of Polymer Chemistry, (Cornell University Press, 1953)
[8] H.G. Elias, Macromolecules, (Wiley-VCH, Weinheim, 2009)
[9] G. S. Grest, L. J. Fetters, J. S. Huang, and D. Richter, Adv. Chem. Phys. 94, 67 (1996)
[10] J. Allgaier, K. Martin, H. J. Räder, and K. Müllen, Macromolecules 32, 3190 (1999)
[11] H.J. Benoît, J. Polym. Sci., 11**,** 507 (1953).
[12] William D. Dozier, John S. Huang, Lewis J. Fetters, Macromolecules 24 2810 (1991)
[13] G. Beaucage, J. Appl. Crystallogr. 28, 717(1995)
[14] J. Stellbrink et al., Applied Physics A 74, S355 (2002)
[15] J. Stellbrink et al. Macromolecules, 31, 4189 (1998)
[16] A.Z. Niu et al., Macromolecules 42 1083 (2009)
[17] I.W. Hamley, The Physics of Block Copolymers; (Oxford University Press: New York, 1998)
[18] M. Antonietti and S. Förster, Vesicles and Liposomes: A Self-Assembly Principle Beyond Lipids, Vol. 15, (WILEY-VCH Weinheim, , 2003)
[19] G. Riess, *Prog. Polym. Sci.* 28, 1107 (2003)
[20] A. Halperin, M. Tirell and T.P. Lodge, *Adv. Polym. Sci.* 100, p31 (1990).
[21] E.B. Zhulina, M. Adam, I. LaRue, S.S. Sheiko, M. Rubinstein, Macromolecules 38, 5330 (2005)
[22] J. Stellbrink, G. Rother, M. Laurati, R. Lund, L. Willner and D. Richter, J. Phys.: Cond. Matter, 16, S3821 (2004)
[23] A. Halperin and S. Alexander, Macromolecules 22, 2403 (1989)
[24] E. Dormidontova, Macromolecules 32, 7630 (1999)
[25] L. Willner, A. Poppe, J. Allgaier, M. Monkenbusch, and D. Richter, Europhys. Lett. 55, 667 (2001)
[26] C.N. Likos et al., Phys. Rev. Letters, 80, 4450, (1998)
[27] M. Watzlawek, C. N. Likos, and H. Lowen, Phys. Rev. Lett. 82, 5289 (1999).
[28] M. Laurati, Phys. Rev. Letters, 94 195504 (2005)
[29] B. Lonetti et al. Phys. Rev. Letters, 106, 228301 (2011)

Exercises

E6.1 Contrast or no contrast?

Due to synthetic (and financial) limitations only protonated material is available for a SANS experiment, for both polymer (poly(ethylene propylene), PEP, and solvent dimethyl-formamide, DMF.

a) Calculate the contrast factor $\frac{\Delta\rho^2}{N_A}$.

b) What is the necessary molecular weight M_w to achieve a signal-to-background ratio of 5 at Q=0 for a given polymer volume fraction ϕ_p =0.01? (Remember: Also the incoherent scattering contributes to the background and there is an empirical "rule of thumb" that the experimental incoherent scattering is twice the theoretical value due to inelastic and multiple scattering!)

c) At which Q-value the signal vanishes in the background?

(Assuming good-solvent conditions with a prefactor 0.01 [nm] for the R_g-M_w-relation and assuming the Guinier approximation for $P(Q)$)

d) For which combination of molecular weight and volume fraction ϕ_p the experiment could be performed in the dilute regime, i.e. $\phi_p \leq 0.1\phi^*$?

Given are sum formulae and densities

h-PEP = C_5H_{10}, d_{PEP}=0.84g/cm^3

h-DMF = C_3H_7NO, d_{PEO}=0.95g/cm^3

and coherent and incoherent scattering lengths b_{coh} and b_{inc} in units [cm]:

C: b_{coh} =6.65E-13, b_{inc} = 0

H: b_{coh} =-3.74E-13, b_{inc} = 2.53E-12

D: b_{coh} =6.67E-13, b_{inc} = 4.04E-13

O: b_{coh} =5.80E-13, b_{inc} = 0

N: b_{coh} =9.36E-13, b_{inc} = 0

E6.2 Contrast factors for Micelles

In aqueous solution, the diblock copolymer poly(ethylene propylene-block-ethylene oxide), PEP-PEO, forms spherical micelles, with PEP the non-soluble and PEO the soluble block. Using SANS combined with contrast variation the micellar structure should be investigated. To prepare the corresponding samples the following parameters have to be calculated

a.) the coherent scattering length densities ρ_{PEP} and ρ_{PEO} in units of [cm^{-2}]:

Known are the monomer sum formulae and densities
h-PEP = C_5H_{10}, d_{PEP}=0.84g/cm^3
h-PEO = C_2H_4O, d_{PEO}=1.12g/cm^3
the degree of polymerisation, D_p, of the blocks:
$D_{p,PEP}$ = 15
$D_{p,PEO}$ = 40
and the coherent scattering lengths b_{coh} in units [cm]:
C=6.65E-13
H=-3.741E-13
D=6.671E-13
O=5.803E-13
b.) the isotopic solvent mixture (H2O/D2O) that match the scattering length density of either PEP and PEO.
Given: d_{D2O}=1.1g/cm^3

E6.3 Aggregation number of micelles

For the same PEP-PEO micelles as in E6.2, in dilute solution using core contrast, i.e. the scattering length density of the solvent is matched to the scattering length density of the micellar shell (formed by the soluble block PEO), the first form factor minimum is observed at Q=0.12 Å^{-1}.
Calculate
a.) the aggregation number N_{agg}, i.e. the number of diblock copolymers forming a single micelle, assuming full segregation, i.e. a non-swollen micellar core.
b.) How can N_{agg} derived in this way be cross-checked without performing another experiment?

E6.4 Reduced forward scattering (virial expansion)

For the same PEP-PEO micelles as in E6.2 at finite concentration using core contrast the corresponding forward scattering *I(Q=0)* for volume fractions ϕ_1=1x10^{-3}, ϕ_2=5x10^{-3} and ϕ_3=7.5x10^{-3} assuming a second virial coefficient A_2=2x10^{-4} should be calculated.

E6.5 Peak position in *S(Q)*

A solution of compact spherical colloids, R=250Å, with volume fraction 0.25 should be characterised by SANS. At which Q-vector do you expect the first peak in the structure factor *S(Q)* to appear?